Variation of lattice dimensions in epitaxial SnS films on MgO(001)

Hiroshi Nozaki*, Mitsuko Onoda, Masamitsu Sekita, Kousuke Kosuda, Toshiaki Wada

National Institute for Materials Science, 1-1 Namiki, Tsukuba, Ibaraki, 305-0044, Japan

Abstract

Epitaxial and polycrystalline SnS films were prepared on MgO(001) and glass substrates using molecular beam epitaxy. The films were characterized by X-ray diffraction method. The orientations of epitaxial films were (010)[100]SnS‖(001)[100]MgO or (010)[001]SnS‖(001)[100]MgO. Lattice parameters of the polycrystalline film closely resembled those of bulk SnS at room temperature. However, the lattice parameters of epitaxial films varied widely and were very different from those of bulk SnS at room temperature. Considering the lattice dimensions and a/c ratio, the films roughly correspond to bulk SnS at elevated temperatures from 371 to 666 K. SEM images of the films showed needle- or circular-like SnS crystallites segregated from the epitaxial films. Respective energies of indirect band gaps of the films and refractive index of the polycrystalline film were estimated using results of optical transmission experiments.
© 2004 Elsevier Inc. All rights reserved.

Keywords: Tin sulfide; Epitaxial films; Molecular beam epitaxy; X-ray diffraction; Magnesium oxide; Lattice parameters; SEM image; Segregation; Band gap; Refractive index

1. Introduction

Lattice dimensions of heteroepitaxial film are modified near the substrate surface as a result of chemical bonding between the film and the substrate surface. The modified lattice dimensions are relaxed to intrinsic ones of the bulk material over critical thickness of the film [1]. However, thick heteroepitaxial films (larger than 100 nm) often have lattice dimensions that differ greatly from those of their bulk materials that are stable at room temperature [2]. In this case, the critical thickness may be very large. Alternatively, metastable crystal structure with vastly different lattice dimensions may be frozen. In the process of preparing SnS films on MgO(001) substrate, we obtained SnS films with lattice dimensions that differed greatly from the bulk material at room temperature. It is expected that production of the films is attributable to a variable nature of chemical bond of SnS, depending on temperature.

The structure of SnS at room temperature is orthorhombic (space group *Pbnm*) with a distorted NaCl-type structure. It has lattice dimensions of $a = 0.4334$ nm, $b = 1.1200$ nm, and $c = 0.3987$ nm at room temperature [3,4]. The structure is characterized by a sequence of double layers of Sn and S atoms that are tightly bound perpendicular to the b-axis. However, chemical bond within the double layers is anisotropic, which results in the anisotropic dimensions a and c, as mentioned above. The double layers bond weakly to adjacent double layers. Thereby, the material is transformed to a high temperature structure (space group *Cmcm*) at 878 K ($a = 0.4148$ nm, $b = 1.1480$ nm, and $c = 0.4177$ nm at 905 K) and the structure change is in second order [5–7]. The a/c ratio of low temperature structure decreases continuously from 1.09 to 0.99 with increasing temperature, where both shorter Sn–S bond length (0.2665 nm) and longer Sn–S bond length (0.3290 nm) at room temperature within the double layer approach to 0.296 nm at 905 K [3,5]. For that reason, the compound can potentially take a wide range of variations of bond length and lattice dimensions,

---

*Corresponding author. Fax: +81 029 852 7449.
E-mail address: nozaki.hiroshi@nims.go.jp (H. Nozaki).

which appears to be advantageous to produce epitaxial films using appropriate substrates.

Epitaxial films have been prepared on NaCl, KCl, and KBr single crystal substrates. Their crystal structures were investigated using electron diffraction method [8,9]. Tin sulfide films with the NaCl type of structure were prepared on NaCl substrates at temperatures above 770 K. Nevertheless further observations regarding tin sulfide films with the NaCl type of structure have not been reported. Polycrystalline SnS films have been prepared using several methods [10–16] for use in potential applications of a compound with strong absorption of visible light and band gap of about 1.1 eV.

The present study prepared epitaxial films on MgO(001) substrates and a polycrystalline film on a glass substrate. Thereafter, we characterized them using X-ray diffraction method. It is noteworthy that the lattice dimension of substrate MgO ($a_{MgO} = 0.4213$ nm) is intermediate between a and c dimensions of SnS, which possibly accommodates a/c of films to the lattice dimension of the substrate. These films had some range of lattice dimensions largely different from those of SnS bulk material at room temperature. Optical properties of the films are also reported.

2. Experimental

These films were prepared by molecular beam epitaxy (MBE). Previous studies have described the experimental setup [2,17]. Substrate temperatures were calibrated using the melting point of Sn. Polished MgO substrates were annealed at 1080 °C in an O_2 atmosphere for 2 h. Crystallographic characteristics and epitaxial orientation of the films were determined using an X-ray diffractometer with a converged X-ray beam, which was described in previous studies [2,17]. The data collection procedure was the same as that performed in those studies. However, a preliminary experiment using X-ray precision method with Ag$K\alpha$ was necessary to elucidate in-plane lattice periodicity because the lattice dimensions of SnS films differed greatly from those of the ordinary bulk SnS reported.

Scanning electron microscope (SEM) images of the films, denoted as F1, F2 and F4–F7 in Table 2 of Section 3.1, were taken by an electron probe microanalyzer (EPMA, JEOL Co. JXA-8500F). Film thickness was determined using a stylus method. Optical transmission measurements of the films were made with a Hitachi U-3500 spectrometer.

3. Results and discussion

3.1. Characterization by X-ray diffraction

An X-ray reflection pattern of the polycrystalline SnS film deposited on glass substrate is shown in Fig. 1,

where the specimen is denoted as F1 in Table 2. Observed reflections, their intensities, and their lattice dimensions almost agree with those of ordinary bulk SnS (JCPDS-ICDD No.14-0620 and Ref. [6]).

Films deposited on polished or cleaved MgO(001) substrates were all grown epitaxially with orientations of [100](010)SnS ∥ [100](001)MgO or [001](010)SnS∥ [100](001)MgO, as mentioned later. A typical X-ray $\theta - 2\theta$ scanning pattern for the epitaxial film F4 is shown in Fig. 2. Reflections $0\,k\,0$ ($k = 2, 4, 8$) are clearly seen in the figure. It indicates the orientation of (010)SnS∥ (001)MgO. There are very weak reflections of 021 and 042 marked by asterisks in the figure. These originate from segregation of SnS crystallites on the film surface and the details are discussed in a later section. X-ray $\theta - 2\theta$ scanning patterns of the other epitaxial films were
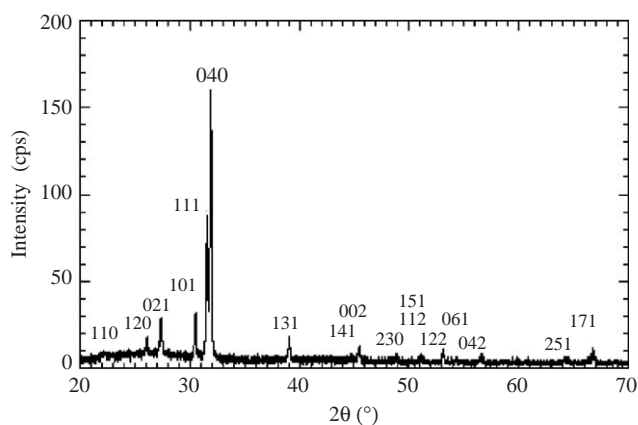

Fig. 1. X-ray $\theta - 2\theta$ scanning pattern of polycrystalline film (F1).
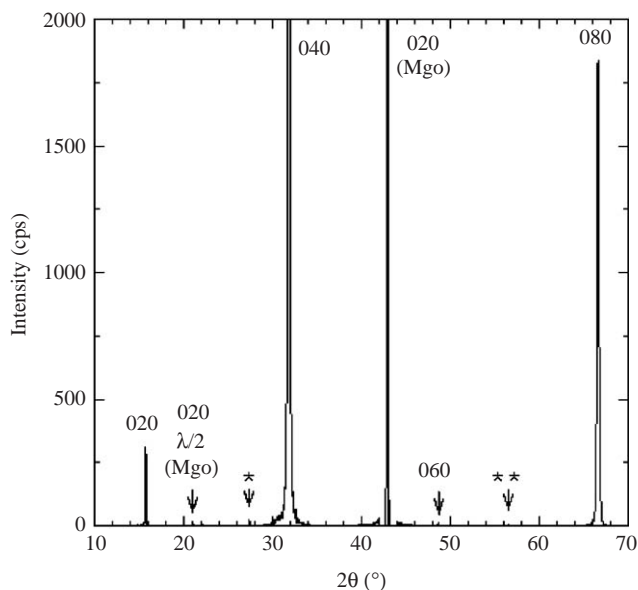

Fig. 2. X-ray $\theta - 2\theta$ scanning pattern of epitaxial film (F4). Reflections marked by asterisks are $0\,1\,2$ and $0\,2\,4$ due to SnS crystallites segregated from the epitaxial film.

essentially the same as that of F4 except for the very weak reflections by the segregation.

X-ray diffraction measurements were performed to obtain reflection data for lattice planes inclined to (010) which is parallel to the substrate surface. If a lattice plane is at an angle α_{ip} with (010) and satisfies the Bragg condition, directions of incident and reflected X-ray beams are asymmetric to the substrate surface, that is, angles of incident and reflected beams with the substrate surface are $\theta_B - \alpha_{ip}$ and $\theta_B + \alpha_{ip}$ (or $\theta_B + \alpha_{ip}$ and $\theta_B - \alpha_{ip}$), respectively, where θ_B is a Bragg angle. Although the substrate body intercepted many reflections with $\theta_B < \alpha_{ip}$ and some others were too weak to

measure, as many X-ray reflections as possible were measured in each film to determine the lattice dimensions precisely by setting the film at appropriate angles of ϕ and Ω rotations for the indicated lattice plane. ϕ is an azimuth angle within the substrate surface and Ω an angle around the θ-axis. Observed d-spacing and intensities of reflections for the F4 specimen are listed in Table 1, where calculated d spacing and interplanar angle α_{ip} are based on the lattice dimensions obtained by the least-squares method. The d-spacing values of the other films were obtained by the same procedure mentioned above. The lattice parameters of the present films are listed in Table 2 together with various experimental conditions for preparation of the films.

3.2. In-plane epitaxy

In-plane epitaxial relation between film and substrate was determined by measuring dependence of 0 8 4 reflection intensity on ϕ-rotation for the F4 film, as shown in Fig. 3. Since the lattice plane (084) intersects (010) with a line parallel to the a-axis, the dependence of 0 8 4 intensity on ϕ-rotation gives the direction of the a-axis within (010). In Fig. 3, ϕ-dependence of 2 0 4 reflection intensity for MgO is also shown. The peak position in the ϕ-dependence of 2 0 4 indicates the direction of [100]MgO within (001)MgO. The ϕ-dependence of 0 8 4 intensity has peak positions at $0°$, $90°$ and $180°$, which indicates in-plane epitaxial relations of [100]SnS||[100]MgO or [001]SnS||[100]MgO. Results of similar measurements for F2, F3 and F5–F7 films were the same as the result for F4. Thus, it is concluded from these results as well as the X-ray $\theta - 2\theta$ scanning patterns that the epitaxial relations of the present films except F1 are (010)SnS||(001)MgO and [100]SnS||[100]MgO or [001]SnS||[100]MgO.

3.3. Variation of lattice parameters

The lattice parameters of the obtained films varied widely, as shown in Table 2. Particularly, the a-dimension listed in Table 2 is in a range between
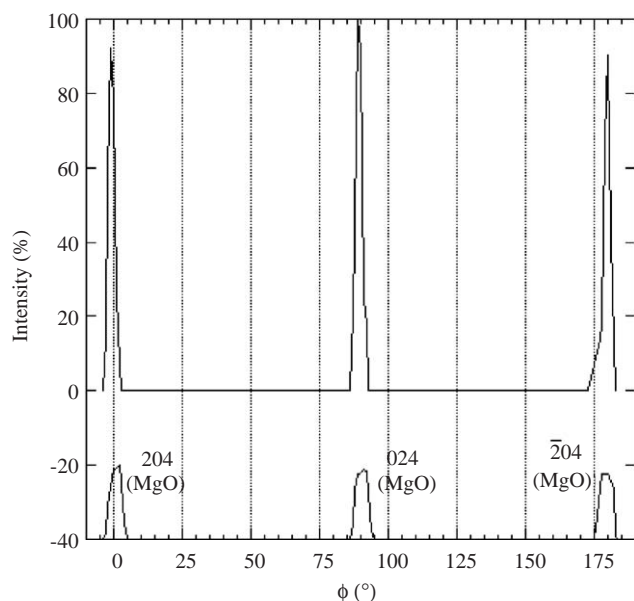
Table 1
Observed and calculated d-spacing, observed intensity, and observed and calculated interplanar angles

h k l	d_{obs} (nm)	d_{cal} (nm)	I_{obs} (%)	α_{obs} ($°$)	α_{cal} ($°$)
0 2 0	0.56002	0.56100	1.2	0.0	0.0
0 4 0	0.28047	0.28050	100.0	0.0	0.0
0 6 0	0.18709	0.18702	<0.1	0.0	0.0
1 6 0	0.17135	0.17129	0.7	23.6	23.7
0 6 1	0.16953	0.16956	0.8	25.0	24.9
1 7 1	0.14063	0.14060	0.7	28.8	28.7
0 8 0	0.14029	0.14025	7.2	0.0	0.0
1 8 0	0.13329	0.13325	1.5	18.1	18.2
0 8 1	0.13245	0.13243	<0.1	19.2	19.2
1 8 1	0.12649	0.12648	0.3	25.7	25.6
2 8 0	0.11726	0.11722	<0.1	33.3	33.3
0 8 2	0.11502	0.11502	0.6	34.9	34.9
1 9 1	0.11475	0.11471	0.4	23.1	23.1
1 10 0	0.10856	0.10852	0.3	14.7	14.7
0 10 1	0.10808	0.10807	0.4	15.6	15.6
2 9 0	0.10759	0.10766	<0.1	30.3	30.3
1 10 1	0.10478	0.10477	<0.1	21.1	21.0
1 11 1	0.096347	0.096327	0.2	19.3	19.2
0 12 0	0.093511	0.093500	0.7	0.0	0.0
2 11 0	0.092063	0.092035	0.1	25.5	25.5
1 12 1	0.089064	0.089074	0.2	17.8	17.7
4 8 0	0.084921	0.084940	<0.1	52.7	52.7
1 13 1	0.082871	0.082791	<0.1	16.5	16.4
0 8 4	0.081694	0.081697	0.2	54.4	54.4
0 14 1	0.078642	0.078596	0.3	11.2	11.3

$a = 0.42696$ nm, $b = 1.1221$ nm and $c = 0.40206$ nm.

Table 2
Lattice parameters and synthetic conditions

Film	a (nm)	b (nm)	c (nm)	a/c	Substrate	Substrate temp. ($°$C)	Deposition rate (nm/m)	Thickness (nm)
F1	0.43290	1.1218	0.39986	1.083	Glass	257–260	2.9	351
F2	0.42804	1.1218	0.39770	1.076	pl-MgO[a]	261–279	3.2	191
F3	0.42636	1.1234	0.40029	1.065	pl-MgO	250–253	—	—
F4	0.42696	1.1221	0.40206	1.062	pl-MgO	333–334	2.2	134
F5	0.42640	1.1229	0.40180	1.061	cl-MgO	257–273	2.4	142
F6	0.42360	1.1261	0.40090	1.057	pl-MgO	253–276	2.7	160
F7	0.42375	1.1254	0.40363	1.050	cl-MgO[a]	262–267	1.1	122

Polished and cleaved MgO substrates are expressed as pl-MgO and cl-MgO, respectively.
[a]Sn was deposited on MgO substrates with nominal thickness of 0.7 nm. The magnitude of a/c for bulk SnS at room temperature is 1.087.

Fig. 3. Intensity dependence of 0 8 4 reflection on ϕ-rotation for epitaxial film (F4) together with that of 0 2 4 reflection for MgO substrate.

0.4236 and 0.4329 nm. The minimum value among them is 2.3% smaller than the a-dimension of bulk SnS at room temperature. The a/c ratio is also in a wide range between 1.050 and 1.083. The dimensions b and c for F7 are 0.5% and 1.2% larger than those of the bulk SnS. However, a polycrystalline film (F1) on a glass substrate had an a/c ratio (1.083) that closely resembled the magnitude (1.087) of bulk SnS at room temperature. Films with a/c around 1.064 were commonly obtained on both polished and cleaved MgO substrates regardless of whether the substrate temperature was high or low, as shown in Table 2. However, deposition was not achieved on a polished MgO substrate at the rather higher temperature of about 400 °C.

We performed Sn deposition (0.7 nm in nominal thickness) prior to SnS deposition experiments for the MgO substrates of F2 and F7 specimens, which yielded SnS films with magnitudes of a/c that differed from those around 1.064. The a/c ratio of F2 is large; it closely resembles that of polycrystalline film F1. The deposited Sn may disturb the lattice periodicity of the MgO substrate surface. It may produce the F2 film with an a/c magnitude closer to that of the polycrystalline film. On the other hand, the a/c ratio of F7 is small and vastly different from the ratios of the bulk and the F1 film. Because there are many steps with various heights on cleaved MgO surface, Sn crystallites may be localized at the steps and may not affect the lattice periodicity of the MgO substrate surface. It is unknown why F7 and F6 films have smaller magnitudes of a/c than those of other epitaxial films. However, we concluded that the lattice periodicity of the surface of MgO substrate

engendered SnS films, which had lattice dimensions that differed greatly from those of bulk SnS at room temperature.

It is necessary to examine the question whether the lattice dimensions of the films are uniform or vary gradually along the direction normal to the substrate surface. The lattice plane (084) of F4 is at 54.4° with (010), as shown in Table 1, and has the maximum interplanar angle among the present observations. Therefore, variation of the c dimension along this direction affects integral breadth of the 0 8 4 reflection. Similarly, the variation of the a dimension along the direction affects the integral breadth of 480 reflection. Integral breadth of the 0 8 4 and 4 8 0 reflections were 0.56° at $2\theta_B = 141.07°$ and 0.68° at $2\theta_B = 130.19°$, respectively. It suggests that variations of interplanar spacing of (084) and (480) along the direction normal to the substrate surface are within $\pm 0.10\%$ and $\pm 0.14\%$ at most, respectively. Integral breadth of 0,12,0 reflection which implied the variation of the b dimension directly was 0.47° at $2\theta_B = 110.91°$. It suggests also that the variation of interplanar spacing of 0,12,0 is within $\pm 0.14\%$ at most. Thus, it appears that the lattice dimensions of F4, which are different greatly from those of bulk SnS at room temperature, maintain almost over the whole volume of the film within the above variations at most.

3.4. Comparison between SnS films and bulk SnS

In order to specify the origin of the lattice dimensions of films that differ largely from those of bulk SnS at room temperature, dependences of lattice parameters (a, $b/(2\sqrt{2}$ and c) on a/c are shown in Fig. 4 together with lattice parameters of bulk SnS at various temperatures
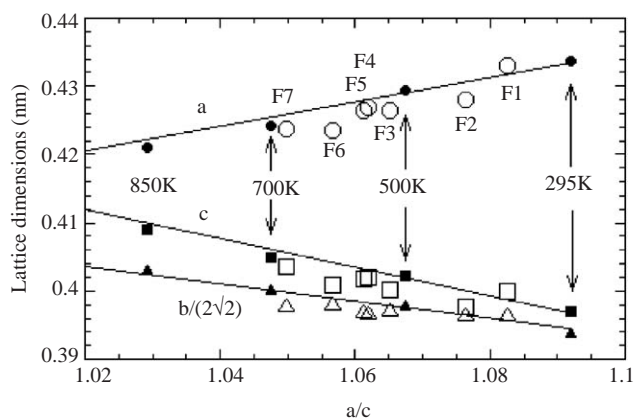

Fig. 4. Dependence of lattice dimensions on a/c. Open circles (a), open triangles ($b/(2\sqrt{2})$), and open squares (c) represent data of the present film. Previous data of temperature dependence of lattice parameters [7] are used to plot dependences of lattice dimensions on a/c which are represented by solid circles (a), solid triangles ($b/(2\sqrt{2})$), and solid squares (c).

[7]. The *a* dimension decreases almost linearly with decreasing a/c, while both dimensions, $b/(2\sqrt{2})$ and *c*, increase slightly with decreasing a/c. Therefore, unit lattice volumes of films except F1 are $0.1918 \pm 0.0008 \, \text{nm}^3$ and almost invariable.

Each lattice parameter of bulk SnS at various temperatures is linearly dependent on a/c in the range between $a/c = 1.029$ and 1.092. Furthermore, the temperatures from 295 to 850 K that are indicated in the figure also have a linear dependence on a/c. Thus, the magnitude of a/c gives a temperature at which bulk SnS exists. Lattice parameters of the present films nearly lie on the linearly dependent lines of bulk SnS. Roughly speaking, therefore, a film with a particular magnitude of a/c corresponds to bulk SnS existing at the temperature indicated by the magnitude of a/c. For example, films F1, F3, and F7 roughly correspond to bulk materials at 371, 532, and 666 K, respectively.

Detailed examination suggests that the lattice parameters of the films deviate slightly from the linearly dependent lines of the bulk material, but those of the polycrystalline film (F1) lie just on the lines. Parameters *a* and *c* of all films except F1 are lower than that of the bulk material. Namely, parameter *a* of the film shifts to that of the bulk material at a higher temperature, while parameter *c* does so at a lower temperature. This fact probably reflects chemical bond characteristics of the material: the parameter of the *a*-axis, along which the weak bond is included, is easily shortened to approach the lattice dimension of MgO substrate, while the parameter of the *c*-axis, along which only the primary bond exists, is hardly extended to the lattice dimension of MgO substrate. Parameter $b/(2\sqrt{2})$ increases very slightly with decreasing a/c because the *b* direction is perpendicular to the substrate surface.

We infer that, in the SnS material, the interfacial interaction between the film and substrate greatly distorts the lattice dimensions of the film, particularly along the weak bond direction, not only near the substrate surface, but over the whole range of the film along the direction perpendicular to the substrate surface.

3.5. SEM images

The present films were all optically reflecting. Morphology of the film surface was investigated by SEM, as shown in Figs. 5a–f. An SEM image for the polycrystalline film (Fig. 5a) indicates that the film consists of aggregate of needle-like crystallites with 100–200 nm in length which are oriented randomly.

The SEM image of the F2 film (Fig. 5b) appears to be similar to that of F1. The a/c ratios of both films are large and close to each other. The X-ray $\theta - 2\theta$ scanning pattern of F2 showed very weak reflections in addition to strong reflections $(0k0)$, as shown in Table 3. The very

weak reflections should not be observed for the film with the epitaxial orientation determined in Section 3.2. Lattice parameters obtained from these reflections were different from those of the F2 epitaxial film and were close to those of the polycrystalline film. Therefore, it is considered naturally that the very weak reflections observed originate from crystallites segregated on the epitaxial film surface and these crystallites give the above SEM image.

The SEM images of F4 and F5 (Figs. 5c and d) were greatly different from each other, although the a/c ratios of both films were almost the same. The surface of the F4 film is mostly filled by circular-like crystallites with 100–300 nm diameter. Since the contrast of the SEM image was very weak, the surface of the film was almost flat. The very weak 0 2 1 and 0 4 2 reflections $(d_{021} = 0.3251 \, \text{nm}$ and $d_{042} = 0.1627 \, \text{nm})$ were observed in the X-ray $\theta - 2\theta$ scanning pattern, as mentioned in Section 3.1. It is also considered that the very weak X-ray reflections and the SEM image of F4 originates from the circular-like crystallites segregated from the epitaxial film. It is presumed that the circular-like crystallites adhere to the epitaxial film surface with the (021) lattice plane because of observation of 0 2 1 and 0 4 2 reflections in the X-ray $\theta - 2\theta$ scanning pattern. The lattice plane (021) consists of alternative layers of sulfur and tin ions. It is noteworthy that the substrate is polished MgO and its temperature on deposition is the highest among the present films.

In contrast with the image of F4, the SEM image of F5 showed that large needle crystallites 200–500 nm in length and clear rectangular shapes were scattered on a flat surface with a weak oriented trend. The substrate was cleaved MgO. These crystallites were also considered to be segregated from the epitaxial film of F5, although no X-ray reflections except 211 for the segregated crystallites were observed in the X-ray $\theta - 2\theta$ scanning pattern.

The SEM images of F6 and F7 (Figs. 5e and f) are magnified three times in comparison with the others. There exist two kinds of needle crystallites in the image of F7. One of them is oriented almost along the $\langle 101 \rangle$ direction of the epitaxial film and has weak contrast. The other has no clear orientation and more bright contrast than that of the former. It appears that the former crystallites adhere more strongly to the epitaxial surface of F7 than the latter ones. Length of both the needle crystallites, 100–200 nm, is shorter than that of the F5 film. As a result of this, their number is about three times larger than that of F5. The lattice plane (101) of SnS with the distorted NaCl-type structure corresponds to (100) of the NaCl-type structure in which cleavage occurs easily. Although (010) is a cleavage plane for SnS, interplanar bonding of (101) lattice planes may be also relatively weak. It is therefore presumed that the segregation of the former needle
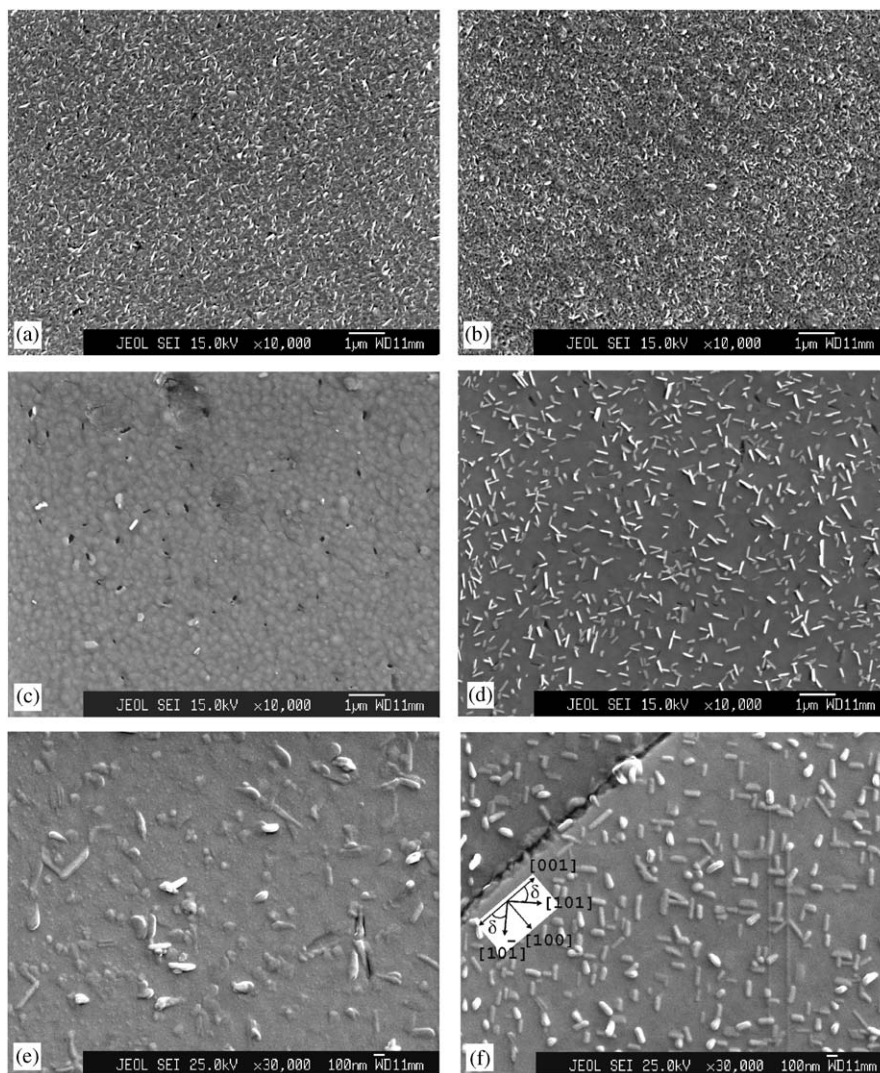
Fig. 5. SEM images of the films, (a) F1, (b) F2, (c) F4, (d) F5, (e) F6, and (f) F7. The direction along step of substrate in (f) is [001] or [100] of the epitaxial film. $\delta = 43.6°$ (or $46.4°$).

Table 3
Observed d-spacing and lattice parameters of crystallites segregated from epitaxial F2 and F7 films

Film name	$h\,k\,l$	d_{obs} (nm)	Film name	$h\,k\,l$	d_{obs} (nm)
F2, $a = 0.4312$ nm, $b = 1.1234$ nm, and $c = 0.3991$ nm	0 2 1	0.32546	F7, $a = 0.4262$ nm, $b = 1.1310$ nm, and $c = 0.3999$ nm	1 2 0	0.34037
	0 0 2	0.19957		0 2 1	0.32650
	2 1 1	0.18704		0 4 2	0.16326
	0 4 2	0.16263			

crystallite occurs along the (010) and (101) lattice planes of the epitaxial film. In contrast with the former, the latter needle crystallites with more bright contrast may adhere to the (010) epitaxial film surface more weakly than the former. Very weak reflections observed in an X-ray $\theta - 2\theta$ scanning pattern are listed in Table 3. X-ray reflections for (120) and (021) were observed there. It is therefore presumed that these reflections may originate from the latter crystallites which connect the (010) epitaxial film surface with (120) or (012) of the crystal-lites. However, more detailed study will be needed to confirm these presumptions. The lattice dimensions of the segregated crystallites are different from those of the epitaxial film F7. The substrate of F7 is cleaved MgO.

The SEM image for F6 shows small circular-like crystallites (20–100 nm in diameter) and relatively large

needle-like ones (200–400 nm in length) segregated from the epitaxial film of F6. It appears to be intermediate between the images of F5 and F7. The number of segregated crystallites is smaller than that in F7. No reflections in the X-ray $\theta - 2\theta$ scanning pattern for the segregated crystallites were observed, which is probably due to a small number of the bright needle crystals, as shown in Fig. 5e. The substrate of F6 is polished MgO.

The SEM images of the present films are dependent upon the substrate surface as well as the a/c ratio, as mentioned above. For example, circular-like crystallites were not observed in the films for the cleaved MgO substrates but in the films for the polished MgO substrates. There exist only needle crystallites in the films with the cleaved MgO substrates. In any cases, it is considered that surfaces of the present films, which have different lattice dimensions from those of bulk SnS at room temperature, are relaxed by the segregation observed in the SEM images.

3.6. Optical properties

Optical transmission experiments for the films were done at room temperature using unpolarized light. Photon energy dependencies of $(\alpha h v)^{1/2}$ for F1, F5, and F7 specimens are shown in Fig. 6. The dependence of F1 specimen, which is the thickest polycrystalline film, shows an interference fringe in the range below 1.7 eV. Extrapolated straight lines through linear dependences from 2 to 1.7 eV intersect the energy axis. The intersection gives the energy of the indirect band gap. The indirect energy gaps of the films are 1.06, 1.13 and 1.09 eV for F5, F1, and F7 specimens, respectively. These values are compared with previous data using thin crystals prepared by cleavage where the plane of cleavage is (010) and incident light is parallel to the b-axis. Albers et al. reported the value of 1.07 ± 0.04 eV that was obtained using unpolarized light [18]. It has been also reported that the anisotropic indirect energy gaps for two different polarizations $\varepsilon\|a$ and $\varepsilon\|c$ are 1.142 and 1.095 eV, respectively, by Lambros et al. [19] and are 1.076 and 1.049 eV, respectively, by Parenteau et al. [20]. Assuming the anisotropy of indirect energy gap between both cases with incident lights parallel and normal to (010), the indirect energy gap of F1 possibly deviates from that for the normal incidence case because of the anisotropy. Therefore, the present values for F5 and F7 should be compared with these previous values and should agree well with the previous value by use of unpolarized light. It may be suggested that a decrease in a/c ratio increases the indirect energy gap of the SnS film and the indirect energy gap measured along directions perpendicular to the b axis is larger than that along the b axis, which has currently been measured with a thin crystal by cleavage.
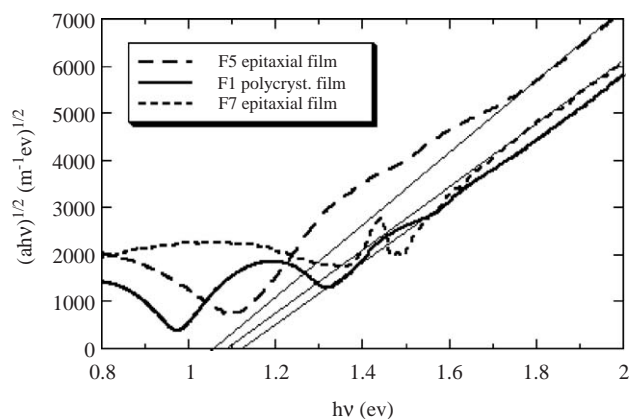

Fig. 6. Square root of the absorption coefficient multiplied by hv dependence on photon energy hv for epitaxial films (F5 and F7) and polycrystalline film (F1).
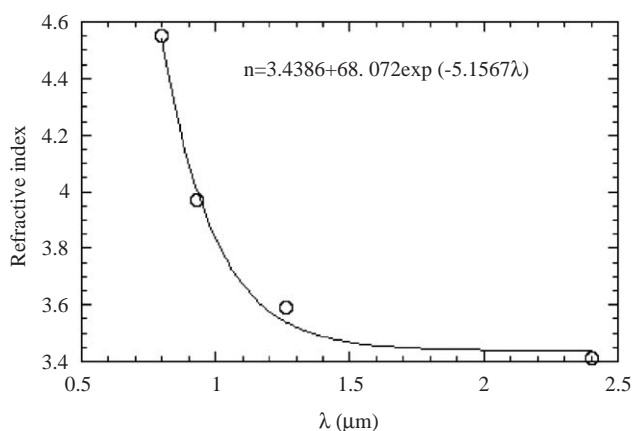

Fig. 7. Refractive index dependence on wavelength for the polycrystalline film (F1).

The refractive index of the F1 specimen was determined from the periodicity of the interference fringe, as shown in Fig. 7 [21]. The refractive index decreases exponentially with increasing wave length; it approaches to a value of 3.4 at an infinite value of wavelength, which agrees fairly well with refractive indexes of 3.503 obtained for $\varepsilon\|a$ and 3.558 for $\varepsilon\|c$ at a long wavelength limit measured at room temperature by Elkorashy [22]. The present magnitude of the refractive index at $\lambda = 1\,\mu m$ is 3.8, which is smaller than values of 4.2 for $\varepsilon\|a$ and 4.5 for $\varepsilon\|c$ measured at 300 K by Lambros et al. [19]. The latter difference may be explainable if one can assume anisotropy of refractive index between both directions normal and parallel to (010).

4. Conclusions

Epitaxial and polycrystalline SnS films were prepared on MgO(001) and glass substrates using MBE. Epitaxial

relations between films and the MgO substrate are [100](010)SnS‖[100](001)MgO or [001](010)SnS‖[100] (001)MgO. Lattice parameters of the films vary widely and differ greatly from those of bulk SnS at room temperature. Dependence of lattice parameters on a/c suggests that the films correspond to bulk SnS existing at temperatures between 371 and 666 K.

The present variable dimensions of lattice parameters are ascribed to the demonstrably variable nature of the bond length of SnS with temperature change and interfacial interaction between the film and the MgO substrate. That interaction largely distorts the lattice dimensions over the whole range of the film along the direction normal to the substrate surface. The SEM images of the films which show SnS crystallites segregated from the epitaxial film are dependent upon the substrate surface as well as the a/c ratio.

The indirect energy gaps of some films and the refractive index of polycrystalline film are presented.

Acknowledgments

References

[1] J.C. Bean, L.C. Feldman, A.T. Fiory, S. Nakahara, K. Robinson, J. Vac. Sci. Technol. A 2 (1984) 436–440.

[2] H. Nozaki, M. Onoda, K. Kurashima, T. Yao, J. Solid State Chem. 157 (2001) 86–93.

[3] H. Wiedemeier, H.G.v. Schnering, Z. Kristallogr. 148 (1978) 295–303.

[4] S.D. Bucchia, J.C. Jumas, M. Maurin, Acta Cryst. B 37 (1981) 1903–1905.

[5] H.G.v. Schnering, H. Wiedemeier, Z. Kristallogr. 156 (1981) 143–150.

[6] H. Wiedemeier, F.J. Csillag, Z. Kristallogr. 149 (1979) 17–29.

[7] T. Chattopadhyay, J. Pannetier, H.G.v. Schnering, J. Phys. Chem. Solids 47 (1986) 879–885.

[8] B.F. Bilenkii, A.G. Mikolaichuk, D.M. Freik, Phys. Status Solidi 28 (1968) K5–K7.

[9] A.G. Mikolaichuk, D.M. Freik, Sov. Phys. Solid State 11 (1970) 2033–2036.

[10] N.K. Reddy, K.T.R. Reddy, Thin Solid Films 325 (1998) 4–6.

[11] B. Thangaraju, P. Kaliannan, J. Phys. D: Appl. Phys. 33 (2000) 1054–1059.

[12] Y. Li, Z. Wang, Y. Ding, Inorg. Chem. 38 (1999) 4737–4740.

[13] M. Jayachandran, S. Mohan, B. Subramanian, C. Sanjeeviraja, V. Ganesan, J. Mater. Sci. Lett. 20 (2000) 381–383.

[14] S. Schlecht, L. Kienle, Inorg. Chem. 40 (2001) 5719–5721.

[15] L.S. Price, I.P. Parkin, A.M.E. Hardy, R.J.H. Clark, T.G. Hibbert, K.C. Molloy, Chem. Mater. 11 (1999) 1792–1799.

[16] T.G. Hibbert, M.F. Mahon, K.C. Molloy, L.S. Price, I.P. Parkin, J. Mater. Chem. 11 (2001) 469–473.

[17] H. Nozaki, M. Onoda, K. Yukino, K. Kurashima, K. Kosuda, H. Maki, S. Hishita, J. Solid State Chem. 177 (2004) 1165–1172.

[18] W. Albers, C. Haas, E. Van Der Maesen, J. Phys. Chem. Solids 15 (1960) 306–310.

[19] A.P. Lambros, D. Geraleas, N.A. Economou, J. Phys. Chem. Solids 35 (1974) 537–541.

[20] M. Parenteau, C. Carlone, Phys. Rev. B 41 (1990) 5227–5234.

[21] R.A. Hazelwood, Thin Solid Films 6 (1970) 329–341.

[22] A.M. Elkorashy, Phys. Status Solidi B 159 (1990) 903–915.